JACS
JOURNAL OF THE AMERICAN CHEMICAL SOCIETY
pubs.acs.org/JACS
Communication

Incorporation of a Phosphino(pyridine) Subcomponent Enables the Formation of Cages with Homobimetallic and Heterobimetallic Vertices

John P. Carpenter,[‡] Tanya K. Ronson,[‡] Felix J. Rizzuto, Théophile Héliot, Peter Grice, and Jonathan R. Nitschke*

Cite This: *J. Am. Chem. Soc.* 2022, 144, 8467−8473
Read Online
ACCESS | Metrics & More | Article Recommendations | Supporting Information

ABSTRACT: Biological systems employ multimetallic assemblies to achieve a range of functions. Here we demonstrate the preparation of metal−organic cages that contain either homobimetallic or heterobimetallic vertices. These vertices are constructed using 2-formyl-6-diphenylphosphinopyridine, which forms ligands that readily bridge between a pair of metal centers, thus enforcing the formation of bimetallic coordination motifs. Two pseudo-octahedral homometallic $M^{I}_{12}L_4$ cages (M^{I} = Cu^{I} or Ag^{I}) were prepared, with a head-to-head configuration of their vertices confirmed by X-ray crystallography and multinuclear NMR for Ag^{I}. The phosphino-pyridine subcomponent also enabled the formation of a class of octanuclear $Cd^{II}_4Cu^{I}_4L_4$ tetrahedral cages, representing an initial example of self-assembled cages containing well-defined heterobimetallic vertices.

Coordination-driven self-assembly provides a powerful tool for the preparation of intricate and functional architectures with relative synthetic ease.[1] The combination of metal ions with well-defined stereoelectronic preferences and ligands that have a rigid arrangement of binding sites has enabled the rational design of polyhedral cage architectures including tetrahedra,[2] cubes,[3] octahedra,[4] and higher-order structures.[5] These cages have attracted considerable interest due to their ability to bind guests within well-defined inner cavities, within which the chemical reactivity and dynamics of guest molecules may be altered.[6]

Most metal−organic cages contain monometallic vertices, as the design principles for these vertices are relatively well-understood. Increased structural complexity and diversity are enabled by the presence of vertices formed from bimetallic units[7] or more complex clusters.[8] Such vertices can also increase the functional complexity, because multiple metal ions can bring about new reactivity.[9] Heterometallic structures[10] are challenging to synthesize in a controlled manner, requiring strategies that include the incorporation of preformed kinetically inert metal−organic building blocks,[11] the use of a mixture of hard and soft ligands that bind different metals preferentially,[12] or the use of ligands with different denticities.[13]

Recently we explored the use of 2-formyl-1,8-napthyridine to prepare cages incorporating disilver vertices.[14] Herein we employ 2-formyl-6-diphenylphosphinopyridine **A**, a subcomponent containing both N and P donors with nonconverging coordination vectors, as a general method for the construction of metal−organic cages having either homobimetallic or heterobimetallic vertices. Subcomponent **A** was previously incorporated into a dicopper(I) motif,[15] which was integrated into extended architectures when flexible dianilines were used in combination with rigid carboxylate templates. We reasoned that the combination of **A** with a more rigid, tritopic aniline would enable the synthesis of more complex metal−organic cages, where the dicopper(I) motif would bring together two aniline residues at the vertices of the cage, without requiring carboxylate templation.

The reaction of **A** (12 equiv), tris(4-aminophenyl)amine **B** (4 equiv), and $[Cu^{I}(MeCN)_4](OTf)$ (12 equiv, $^{-}$OTf = trifluoromethanesulfonate, triflate)[16] led to the formation of $Cu^{I}_{12}L_4$ cage **1** (Figure 1a), the composition of which was confirmed by ESI-MS. The ^{1}H NMR spectrum of **1** indicated the formation of a high-symmetry product in solution, with the ligand in an environment having 3-fold symmetry. ^{1}H DOSY NMR further confirmed that the aromatic signals corresponded to a single species (Figure 1b).

The crystal structure of **1** revealed a pseudo-octahedral geometry, with a pair of Cu^{I} ions occupying each vertex (Figure 1c). Four faces of the octahedron are occupied by tritopic ligands, while the remaining faces are vacant.[4] Each dimetallic vertex has the same *P* or *M* helical twist, with the assembly expressing approximate *T* point symmetry, consistent with the solution NMR spectra. Both cage enantiomers were observed in the crystal.[17]

The bimetallic vertices display a head-to-head configuration, rather than adopting the head-to-tail arrangement observed in other structures incorporating **A**[15] and related dicopper(I) complexes[18] (Figure 1b and d). The internal Cu^{I} ion of each

Received: February 28, 2022
Published: May 5, 2022

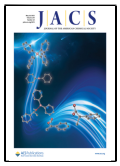

https://doi.org/10.1021/jacs.2c02261
J. Am. Chem. Soc. 2022, 144, 8467−8473

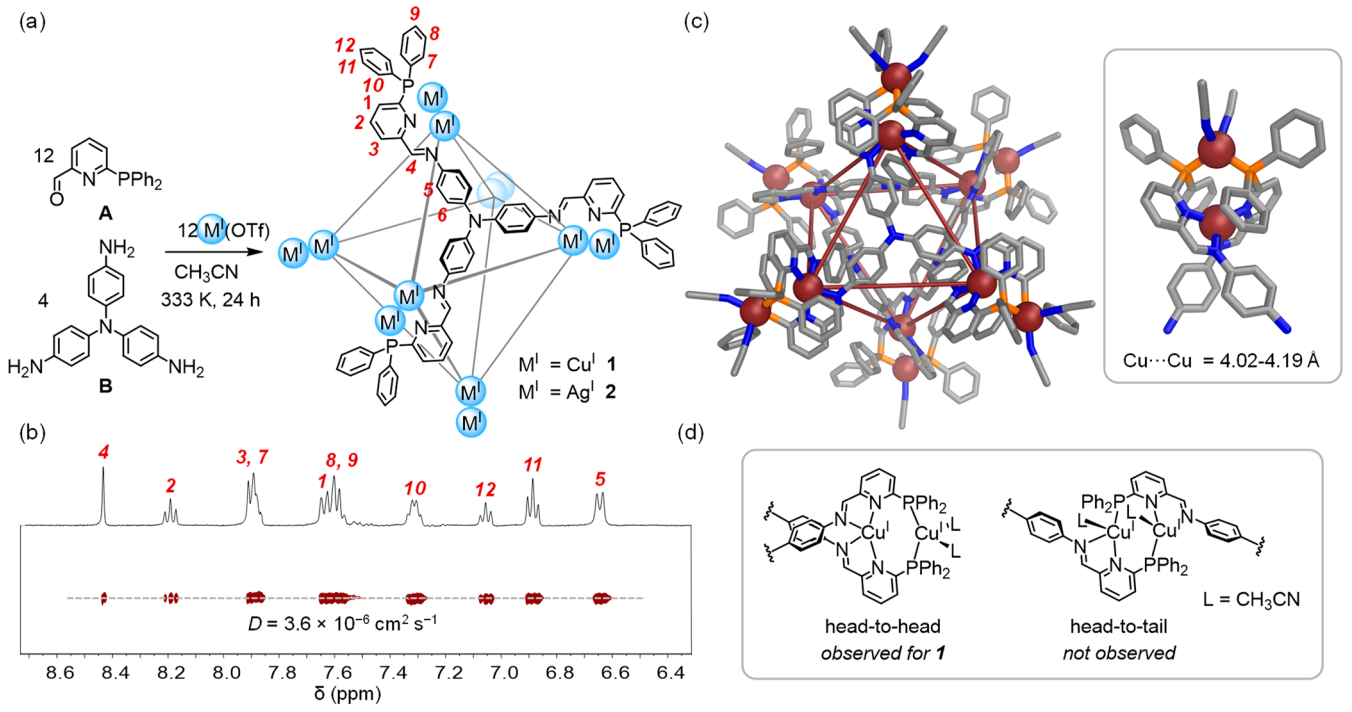

Figure 1. (a) Subcomponent self-assembly of $M^{I}_{12}L_4$ cages **1** and **2**. Externally coordinated acetonitrile molecules are omitted for clarity. (b) ^{1}H and DOSY NMR spectra of **1**. The signal for H_6 is not observed at 298 K (see Supporting Information Section 1.2).[19] (c) Crystal structure of **1** with inset showing one of its dicopper(I) vertices. Disorder, anions, solvent of crystallization, and hydrogen atoms are omitted for clarity. (d) Illustration of the head-to-head vertex geometry observed for **1** and the alternative head-to-tail arrangement previously observed in analogous dinuclear Cu^I complexes.[15]

vertex is thus chelated by two pyridyl-imine units, and the outer Cu^I ions are coordinated by two phosphine donors with a further two external acetonitrile molecules completing their tetrahedral coordination spheres. We infer that this arrangement is more favorable than a counterfactual structure with head-to-tail vertices, where the additional acetonitrile ligands would be left inside the cavity to engender steric crowding (see Supporting Information Section 3).

The coordination environments of the inner Cu^I ions are distorted from a regular tetrahedral geometry, with angles of 66.2−70.4° between the two pyridyl-imine chelate planes and N−Cu^I−N angles in the range 80.3−139.5°. The outer Cu^I ions display a more regular tetrahedral geometry, with angles of 97.9−116.9° between ligands. The metal centers of each vertex are separated by 4.02−4.18 Å (average = 4.10 Å), which is much greater than twice the copper(I) van der Waals radius of 1.40 Å,[20] indicating the absence of Cu^I···Cu^I interactions.

The inner Cu^I ions form a regular octahedral framework with an average distance of 12.0 Å along the edges and 16.9 Å between antipodal Cu^I ions. The cavity of **1** encapsulates a single acetonitrile molecule in the solid state. Its volume was calculated to be 90 Å^3 using Molovol.[21]

We reasoned that silver(I) might also form pseudo-octahedral assemblies analogous to **1**, as Ag^I and Cu^I have similar coordination preferences.[22] Furthermore, ^{109}Ag NMR spectroscopy[23] provides a complementary means to characterize coordination complexes incorporating diamagnetic Ag^I in solution.[24] Silver(I) complex **2** was thus formed by treating triamine **B** (4 equiv) with **A** (12 equiv) and Ag^IOTf (12 equiv) (Figure 1a). Its $Ag^I_{12}L_4$ composition was confirmed by ESI-MS, and its ^{1}H NMR spectrum (Figure 2c) was again consistent with a high-symmetry structure in solution.

The crystal structure of **2** confirmed the presence of a pseudo-octahedral assembly (Figure 2a), analogous to **1**, this time with crystallographic *T*-symmetry. The metal−metal separation at each disilver(I) vertex was found to be 3.38 Å, significantly shorter than the average metal−metal distance of 4.10 Å observed for **1** and slightly greater than twice the van der Waals radius of Ag^I (1.66 Å).[20] The inner Ag^I ions form a perfect octahedron with 12.2 Å edges and a distance of 17.3 Å between opposing vertices. The cavity of 69 Å^3 (calculated with Molovol[21]) is slightly smaller than that of **1**, reflecting a more compressed structure.

The inner Ag^I ions, once more coordinated by two pyridyl-imine units, are even more distorted from regular tetrahedral geometry (62.6° between pyridyl-imine chelate planes and N−Ag^I−N angles of 71.1−157.8°) relative to the inner Cu^I ions of **1**, consistent with the greater flexibility of the coordination sphere of silver(I).[25] The outer Ag^I ion of each vertex is coordinated by a single acetonitrile molecule in an approximately trigonal planar coordination geometry (Figure 2b). The coordinated acetonitriles were not observed by ^{1}H NMR, presumably due to rapid exchange with CD_3CN.

The solution structure of **2** was further probed through multinuclear NMR experiments (Figure 2c−e), which confirmed the presence of two distinct Ag^I environments, corresponding to the inner and outer silver ions at each vertex. These data indicate that the solution structure mirrors the solid-state one. The imine signal in the ^{1}H NMR spectrum of **2** split into a doublet (Figure 2d), in contrast to the singlet observed for **1**. In the case of **2**, coupling arises between the imine proton and the nearby internal Ag^I ion with a ^{109}Ag chemical shift of 544 pm, as determined from a ^{1}H−^{109}Ag HMBC spectrum (Figure 2c).[26]

https://doi.org/10.1021/jacs.2c02261
J. Am. Chem. Soc. 2022, 144, 8467−8473

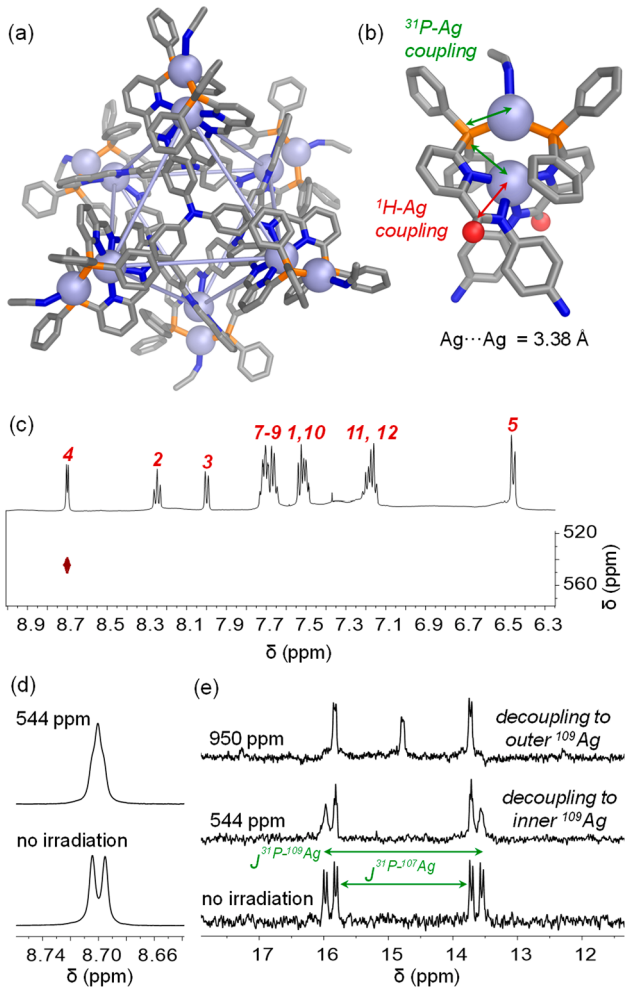

Figure 2. (a) Crystal structure of **2**. Disorder, anions, solvent of crystallization, and hydrogen atoms are omitted for clarity. (b) View of one of the disilver vertices of **2**, with the imine hydrogens shown as red spheres. The observed ^{1}H−Ag and ^{31}P−Ag couplings are highlighted by red and green arrows, respectively. (c) ^{1}H−^{109}Ag HMBC of **2**, revealing a correlation between the imine resonance and the inner silver ions, which resonate at 544 ppm. (d) Coalescence of the imine signal in the ^{1}H NMR spectrum of **2** upon irradiation of ^{109}Ag at 544 ppm. (e) ^{31}P NMR spectra of **2** before and after irradiation of ^{109}Ag at 544 or 950 ppm, resulting in decoupling to the inner and outer ^{109}Ag, respectively.

The ^{31}P NMR spectra of **2** (Figure 2e) showed complex splitting patterns, consistent with coupling between the phosphine and both unique Ag^{I} ions. A major coupling was observed to the external Ag^{I} ions, with further fine splitting resulting from longer-range coupling to the internal Ag^{I} ion, which partially collapsed upon irradiation of the inner ^{109}Ag resonance at 544 ppm. Stimulation of ^{109}Ag over a broad window in approximately 50 ppm increments (Figure S25) allowed identification of a resonance at ca. 950 ppm, corresponding to the outer Ag^{I} ions.

Because structures **1** and **2** possess two distinct coordination environments, we hypothesized that subcomponent **A** might also be capable of stabilizing assemblies with heterobimetallic vertices. We initially investigated whether Cu^{I} and Ag^{I} could be selectively incorporated into the two distinct binding sites at the vertices of the pseudo-octahedral framework shared by **1** and **2**. However, the reaction of trianiline **B** (4 equiv) and **A** (12 equiv) with equimolar amounts of $[Cu^{I}(MeCN)_4](OTf)$ and $Ag^{I}OTf$ (6 equiv each) led to the formation of a distribution of $Cu^{I}_{x}Ag^{I}_{(12-x)}L_4$ pseudo-octahedral species (Figure S26). We infer that the similarity in coordinative preferences between Cu^{I} and Ag^{I} led to the formation of these mixed-metal species.

We hypothesized that a metal ion with different coordinative preferences, such as cadmium(II), would lead to discrimination between the different binding sites when combined with copper(I). The self-assembly of triamine **B** (4 equiv) and **A** (12 equiv) with $[Cu^{I}(MeCN)_4](ClO_4)$ (4 equiv) and $Cd^{II}(ClO_4)_2$ (4 equiv) gave rise to a new product (**3**), which displayed a single ^{1}H NMR signal for each type of ligand proton (Figure 3a).[27] ESI-MS revealed a $Cd^{II}_4Cu^{I}_4L_4$ composition, distinct from pseudo-octahedral assemblies **1** and **2**.

Single-crystal X-ray analysis confirmed the face-capped tetrahedral structure of **3** (Figure 3c). The heterobimetallic vertices of **3** each consist of an inner Cd^{II} and an outer Cu^{I}, separated by distances of 3.47−3.57 Å (average 3.52 Å), greater than the sum of the van der Waals radii of the two ions (2.98 Å).[20] This vertex geometry enables aromatic stacking to occur between a phosphorus-bound phenyl ring from each ligand and the pyridine of a neighboring ligand, with distances of 3.1−3.4 Å between stacked rings (Figure 3c, inset). Such stacking was not observed in the homobimetallic vertices of **1** and **2**.

The Cd^{II} ions bring together three pyridyl-imine ligands at each vertex. The resulting coordination geometry is flattened from a regular octahedral arrangement, with N−Cd^{II}−N angles of 71.5−112.0° between *cis*-coordinated nitrogen donors. The Cu^{I} ions are coordinated by a phosphine donor from each ligand, with a single acetonitrile molecule completing the tetrahedral coordination sphere.

Coordination of Cd^{II} to the pyridyl-imine donors within **3** allows them to adopt their preferred six-coordinate configuration, leaving the phosphine donors free to bind Cu^{I} in an approximately tetrahedral configuration. Although both metal ions are classed as soft acids, the lower charge of Cu^{I} renders it softer than Cd^{II}, and thus with a greater propensity to coordinate to the softer phosphine donors.[28]

The structure of **3** evokes previously reported $M^{II}_4L_4$ tetrahedra,[2a,29] with all octahedral Cd^{II} ions within each cage sharing the same Δ or Λ stereochemistry, and the face-capping ligands also adopting a propeller-like helical arrangement. The Cd^{II} ions are separated by an average distance of 12.6 Å. A cavity volume of 51 Å^3 was calculated using Molovol,[21] within the range observed for analogous tetrahedral cages assembled from **B**, 2-formylpyridine, and Fe^{II} or Co^{II} (31 and 63 Å^3 respectively, calculated using the same method).[2a,29] The central nitrogen atoms of each ligand are slightly pyramidalized to point outward, with C−N−C angles ranging from 115.1° to 118.1° (average 117.3°). This observation contrasts with the structures of **1** and **2**, where the central nitrogen atoms are nearly planar, with average C−N−C angles of 119° and 120°, respectively.

To investigate the generality of this approach for forming heterometallic cages, we also prepared a larger tetrahedral cage based on triamine **C**, which was shown to produce $M^{II}_4L_4$ tetrahedra with rich host−guest chemistry.[2b] Treatment of subcomponents **C** (4 equiv) and **A** (12 equiv) with $[Cu^{I}(MeCN)_4](ClO_4)$ (4 equiv) and $Cd^{II}(ClO_4)_2$ (4 equiv) yielded $Cd^{II}_4Cu^{I}_4L_4$ structure **4** (Figure 3b), as confirmed by

https://doi.org/10.1021/jacs.2c02261
J. Am. Chem. Soc. 2022, 144, 8467−8473

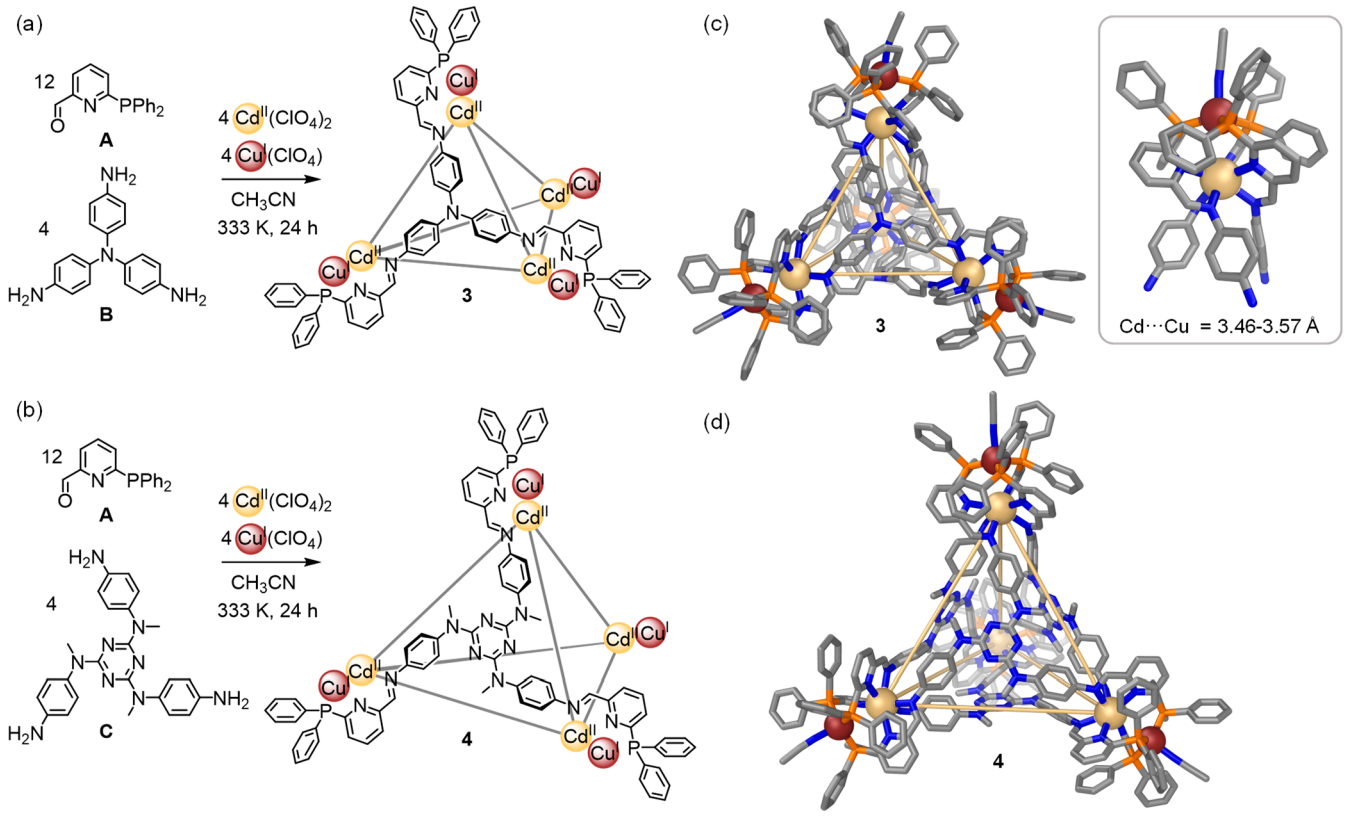

Figure 3. Subcomponent self-assembly of $Cd^{II}_4Cu^{I}_4L_4$ cages (a) **3** and (b) **4**. Externally coordinated acetonitrile molecules are omitted for clarity. (c) Crystal structure of **3** with inset showing one $Cd^{II}Cu^{I}$ vertex. (d) Crystal structure of **4**. Disorder, anions, solvent of crystallization, and hydrogen atoms are omitted for clarity.

ESI-MS. ^{1}H NMR spectra were again consistent with a *T*-symmetric structure in solution.

The crystal structure of **4** confirmed the formation of a face-capped tetrahedral cage with heterobimetallic $Cd^{II}Cu^{I}$ vertices, similar to those of **3** (Figure 3d). The internal Cd^{II} cations are separated from one another by an average distance of 16.3 Å, greater than in **3**, and the 240 Å^3 cavity of **4** is also correspondingly larger, calculated using Molovol.[21] Future work will compare the guest encapsulation abilities of this cavity with that of the analogous $M^{II}_4L_4$ tetrahedron.

Subcomponent **A** represents a rare example of a building block that can generate either homobimetallic or heterobimetallic coordination motifs, resulting in two structurally distinct families of coordination cages. The two chemically distinct coordination environments formed from the previously unreported head-to-head arrangement of **A** have enabled access to cages with heterobimetallic vertices for the first time. Future work will investigate whether the labile coordination sites of the cages, occupied by acetonitrile molecules in the solid state, could enable further functionalization of the cage exterior, to allow tuning of their solubility,[30] the attachment of fluorescent tags for biomedical applications,[31] or the chirality of the cages to be controlled.[32] Explorations may also be fruitful of the mutual influences of the two vertex metal ions, bound at well-defined distances from each other, on the electrochemical properties of the cages and their host–guest properties. Future studies will also seek to exploit the potential photophysical properties[33] of the copper(I)-based cages reported herein for sensing or optoelectronic applications.[34]

■ ASSOCIATED CONTENT

Supporting Information

The Supporting Information is available free of charge at https://pubs.acs.org/doi/10.1021/jacs.2c02261.

Detailed descriptions of synthetic procedures; characterization of new compounds; spectroscopic data (PDF)

Accession Codes

CCDC 2153619–2153622 and 2163435 contain the supplementary crystallographic data for this paper. These data can be obtained free of charge via www.ccdc.cam.ac.uk/data_request/cif, or by emailing data_request@ccdc.cam.ac.uk, or by contacting The Cambridge Crystallographic Data Centre, 12 Union Road, Cambridge CB2 1EZ, UK; fax: +44 1223 336033.

■ AUTHOR INFORMATION

Corresponding Author

Jonathan R. Nitschke − *Department of Chemistry, University of Cambridge, Cambridge CB2 1EW, United Kingdom;* orcid.org/0000-0002-4060-5122; Email: jrn34@cam.ac.uk

Authors

John P. Carpenter − *Department of Chemistry, University of Cambridge, Cambridge CB2 1EW, United Kingdom*

Tanya K. Ronson − *Department of Chemistry, University of Cambridge, Cambridge CB2 1EW, United Kingdom;* orcid.org/0000-0002-6917-3685

Felix J. Rizzuto − *Department of Chemistry, University of Cambridge, Cambridge CB2 1EW, United Kingdom;* Present Address: School of Chemistry, University of New South

Wales, Sydney, 2052, Australia; orcid.org/0000-0003-2799-903X
Théophile Héliot − *Department of Chemistry, University of Cambridge, Cambridge CB2 1EW, United Kingdom*
Peter Grice − *Department of Chemistry, University of Cambridge, Cambridge CB2 1EW, United Kingdom;* orcid.org/0000-0003-4658-4534

Complete contact information is available at: https://pubs.acs.org/10.1021/jacs.2c02261

Author Contributions

‡J.P.C. and T.K.R. contributed equally.

Notes

The authors declare no competing financial interest.

■ ACKNOWLEDGMENTS

This work was supported by the European Research Council (695009), the UK Engineering and Physical Sciences Research Council (EPSRC, EP/P027067/1 and EP/T031603/1), and a Marie Curie Fellowship for J.P.C. (ITN-2010-264645). F.J.R. acknowledges Cambridge Australia Scholarships and the Cambridge Trust for Ph.D. funding. We thank the EPSRC National Mass Spectrometry Centre (Swansea, UK) for high-resolution mass spectrometry and Diamond Light Source (UK) for synchrotron beamtime on I19 (MT15768). We also thank the NMR service team at the Department of Chemistry, University of Cambridge, for performing some NMR experiments.

■ REFERENCES

(1) (a) Ward, M. D. Polynuclear coordination cages. *Chem. Commun.* **2009**, 4487−4499. (b) Pullen, S.; Tessarolo, J.; Clever, G. H. Increasing structural and functional complexity in self-assembled coordination cages. *Chem. Sci.* **2021**, *12*, 7269−7293. (c) Gao, W.-X.; Feng, H.-J.; Guo, B.-B.; Lu, Y.; Jin, G.-X. Coordination-Directed Construction of Molecular Links. *Chem. Rev.* **2020**, *120*, 6288−6325. (d) Cook, T. R.; Stang, P. J. Recent Developments in the Preparation and Chemistry of Metallacycles and Metallacages via Coordination. *Chem. Rev.* **2015**, *115*, 7001−7045. (e) Yoshizawa, M.; Catti, L. Bent Anthracene Dimers as Versatile Building Blocks for Supramolecular Capsules. *Acc. Chem. Res.* **2019**, *52*, 2392−2404.

(2) (a) Bilbeisi, R. A.; Clegg, J. K.; Elgrishi, N.; de Hatten, X.; Devillard, M.; Breiner, B.; Mal, P.; Nitschke, J. R. Subcomponent self-assembly and guest-binding properties of face-capped $Fe_4L_4^{8+}$ capsules. *J. Am. Chem. Soc.* **2012**, *134*, 5110−5119. (b) Bolliger, J. L.; Ronson, T. K.; Ogawa, M.; Nitschke, J. R. Solvent Effects upon Guest Binding and Dynamics of a $Fe^{II}_4L_4$ Cage. *J. Am. Chem. Soc.* **2014**, *136*, 14545−14553. (c) Yan, L.-L.; Tan, C.-H.; Zhang, G.-L.; Zhou, L.-P.; Bünzli, J.-C.; Sun, Q.-F. Stereocontrolled Self-Assembly and Self-Sorting of Luminescent Europium Tetrahedral Cages. *J. Am. Chem. Soc.* **2015**, *137*, 8550−8555. (d) Yi, S.; Brega, V.; Captain, B.; Kaifer, A. E. Sulfate-templated self-assembly of new M_4L_6 tetrahedral metal organic cages. *Chem. Commun.* **2012**, *48*, 10295−10297. (e) Frischmann, P. D.; Kunz, V.; Stepanenko, V.; Würthner, F. Subcomponent Self-Assembly of a 4 nm M_4L_6 Tetrahedron with Zn^{II} Vertices and Perylene Bisimide Dye Edges. *Chem.—Eur. J.* **2015**, *21*, 2766−2769.

(3) (a) Otte, M.; Kuijpers, P. F.; Troeppner, O.; Ivanović-Burmazović, I.; Reek, J. N. H.; de Bruin, B. Encapsulation of Metalloporphyrins in a Self-Assembled Cubic M_8L_6 Cage: A New Molecular Flask for Cobalt−Porphyrin-Catalysed Radical-Type Reactions. *Chem.—Eur. J.* **2013**, *19*, 10170−10178. (b) Yang, L.; Jing, X.; He, C.; Chang, Z.; Duan, C. Redox-Active M_8L_6 Cubic Hosts with Tetraphenylethylene Faces Encapsulate Organic Dyes for Light-Driven H_2 Production. *Chem.—Eur. J.* **2016**, *22*, 18107−18114.

(4) (a) Rizzuto, F. J.; Wu, W. Y.; Ronson, T. K.; Nitschke, J. R. Peripheral Templation Generates an $M^{II}_6L_4$ Guest-Binding Capsule. *Angew. Chem., Int. Ed.* **2016**, *55*, 7958−7962. (b) Fujita, M.; Oguro, D.; Miyazawa, M.; Oka, H.; Yamaguchi, K.; Ogura, K. Self-assembly of ten molecules into nanometre-sized organic host frameworks. *Nature* **1995**, *378*, 469−471. (c) He, C.; Lin, Z.; He, Z.; Duan, C.; Xu, C.; Wang, Z.; Yan, C. Metal-Tunable Nanocages as Artificial Chemosensors. *Angew. Chem., Int. Ed.* **2008**, *47*, 877−881.

(5) (a) Chen, Y.-S.; Solel, E.; Huang, Y.-F.; Wang, C.-L.; Tu, T.-H.; Keinan, E.; Chan, Y.-T. Chemical mimicry of viral capsid self-assembly via corannulene-based pentatopic tectons. *Nat. Commun.* **2019**, *10*, 3443. (b) Pasquale, S.; Sattin, S.; Escudero-Adán, E. C.; Martínez-Belmonte, M.; de Mendoza, J. Giant regular polyhedra from calixarene carboxylates and uranyl. *Nat. Commun.* **2012**, *3*, 785.

(6) (a) Brown, C. J.; Toste, F. D.; Bergman, R. G.; Raymond, K. N. Supramolecular catalysis in metal-ligand cluster hosts. *Chem. Rev.* **2015**, *115*, 3012−3035. (b) Fang, Y.; Powell, J. A.; Li, E.; Wang, Q.; Perry, Z.; Kirchon, A.; Yang, X.; Xiao, Z.; Zhu, C.; Zhang, L.; Huang, F.; Zhou, H. C. Catalytic reactions within the cavity of coordination cages. *Chem. Soc. Rev.* **2019**, *48*, 4707−4730. (c) Wang, K.; Jordan, J. H.; Hu, X. Y.; Wang, L. Supramolecular strategies for controlling reactivity within confined nanospaces. *Angew. Chem., Int. Ed.* **2020**, *59*, 13712−13721. (d) Sinha, I.; Mukherjee, P. S. Chemical Transformations in Confined Space of Coordination Architectures. *Inorg. Chem.* **2018**, *57*, 4205−4221. (e) Saha, R.; Devaraj, A.; Bhattacharyya, S.; Das, S.; Zangrando, E.; Mukherjee, P. S. Unusual Behavior of Donor−Acceptor Stenhouse Adducts in Confined Space of a Water-Soluble Pd^{II}_8 Molecular Vessel. *J. Am. Chem. Soc.* **2019**, *141*, 8638−8645. (f) Horiuchi, S.; Murase, T.; Fujita, M. Noncovalent Trapping and Stabilization of Dinuclear Ruthenium Complexes within a Coordination Cage. *J. Am. Chem. Soc.* **2011**, *133*, 12445−12447.

(7) (a) Eddaoudi, M.; Kim, J.; Wachter, J. B.; Chae, H. K.; O'Keeffe, M.; Yaghi, O. M. Porous Metal−Organic Polyhedra: 25 Å Cuboctahedron Constructed from 12 $Cu_2(CO_2)_4$ Paddle-Wheel Building Blocks. *J. Am. Chem. Soc.* **2001**, *123*, 4368−4369. (b) Li, J.-R.; Zhou, H.-C. Bridging-ligand-substitution strategy for the preparation of metal−organic polyhedra. *Nat. Chem.* **2010**, *2*, 893−898. (c) Jiang, X.-F.; Hau, F. K.-W.; Sun, Q.-F.; Yu, S.-Y.; Yam, V. W.-W. From $\{Au^I\cdots Au^I\}$-Coupled Cages to the Cage-Built 2-D $\{Au^I\cdots Au^I\}$ Arrays: $Au^I\cdots Au^I$ Bonding Interaction Driven Self-Assembly and Their Ag^I Sensing and Photo-Switchable Behavior. *J. Am. Chem. Soc.* **2014**, *136*, 10921−10929.

(8) (a) Liu, G.; Ju, Z.; Yuan, D.; Hong, M. In Situ Construction of a Coordination Zirconocene Tetrahedron. *Inorg. Chem.* **2013**, *52*, 13815−13817. (b) Augustyniak, A. W.; Fandzloch, M.; Domingo, M.; Łakomska, I.; Navarro, J. A. R. A vanadium(IV) pyrazolate metal−organic polyhedron with permanent porosity and adsorption selectivity. *Chem. Commun.* **2015**, *51*, 14724−14727. (c) Howlader, P.; Mukherjee, P. S. Face and edge directed self-assembly of Pd_{12} tetrahedral nano-cages and their self-sorting. *Chem. Sci.* **2016**, *7*, 5893−5899. (d) Wang, L.-J.; Li, X.; Bai, S.; Wang, Y.-Y.; Han, Y.-F. Self-Assembly, Structural Transformation, and Guest-Binding Properties of Supramolecular Assemblies with Triangular Metal−Metal Bonded Units. *J. Am. Chem. Soc.* **2020**, *142*, 2524−2531. (e) Liu, M.; Liao, W.; Hu, C.; Du, S.; Zhang, H. Calixarene-Based Nanoscale Coordination Cages. *Angew. Chem., Int. Ed.* **2012**, *51*, 1585−1588.

(9) (a) Hardy, M.; Lützen, A. Better Together: Functional Heterobimetallic Macrocyclic and Cage-like Assemblies. *Chem.—Eur. J.* **2020**, *26*, 13332−13346. (b) Li, F.; Lindoy, L. F. Metalloligand Strategies for Assembling Heteronuclear Nanocages − Recent Developments. *Aust. J. Chem.* **2019**, *72*, 731−741.

(10) Gao, W.-X.; Zhang, H.-N.; Jin, G.-X. Supramolecular catalysis based on discrete heterometallic coordination-driven metallacycles and metallacages. *Coord. Chem. Rev.* **2019**, *386*, 69−84.

(11) (a) Li, K.; Zhang, L.-Y.; Yan, C.; Wei, S.-C.; Pan, M.; Zhang, L.; Su, C.-Y. Stepwise Assembly of $Pd_6(RuL_3)_8$ Nanoscale Rhombododecahedral Metal−Organic Cages via Metalloligand Strategy for Guest Trapping and Protection. *J. Am. Chem. Soc.* **2014**, *136*, 4456−4459. (b) Wragg, A. B.; Metherell, A. J.; Cullen, W.; Ward, M. D.

Stepwise assembly of mixed-metal coordination cages containing both kinetically inert and kinetically labile metal ions: introduction of metal-centred redox and photophysical activity at specific sites. *Dalton Trans* **2015**, *44*, 17939−17949. (c) Sanz, S.; O'Connor, H. M.; Pineda, E. M.; Pedersen, K. S.; Nichol, G. S.; Mønsted, O.; Weihe, H.; Piligkos, S.; McInnes, E. J. L.; Lusby, P. J.; Brechin, E. K. $[Cr^{III}_8M^{II}_6]^{12+}$ Coordination Cubes (M^{II}=Cu, Co). *Angew. Chem., Int. Ed.* **2015**, *54*, 6761−6764. (d) Luis, E. T.; Iranmanesh, H.; Arachchige, K. S. A.; Donald, W. A.; Quach, G.; Moore, E. G.; Beves, J. E. Luminescent Tetrahedral Molecular Cages Containing Ruthenium(II) Chromophores. *Inorg. Chem.* **2018**, *57*, 8476−8486. (e) Lisboa, L. S.; Findlay, J. A.; Wright, L. J.; Hartinger, C. G.; Crowley, J. D. A Reduced-Symmetry Heterobimetallic $[PdPtL_4]^{4+}$ Cage: Assembly, Guest Binding, and Stimulus-Induced Switching. *Angew. Chem., Int. Ed.* **2020**, *59*, 11101−11107. (f) Preston, D.; Sutton, J. J.; Gordon, K. C.; Crowley, J. D. A Nona-nuclear Heterometallic Pd_3Pt_6 "Donut"-Shaped Cage: Molecular Recognition and Photocatalysis. *Angew. Chem., Int. Ed.* **2018**, *57*, 8659−8663.

(12) (a) Wu, H.-B.; Wang, Q.-M. Construction of Heterometallic Cages with Tripodal Metalloligands. *Angew. Chem., Int. Ed.* **2009**, *48*, 7343−7345. (b) Duriska, M. B.; Neville, S. M.; Moubaraki, B.; Cashion, J. D.; Halder, G. J.; Chapman, K. W.; Balde, C.; Letard, J.-F.; Murray, K. S.; Kepert, C. J.; Batten, S. R. A nanoscale molecular switch triggered by thermal, light, and guest perturbation. *Angew. Chem., Int. Ed.* **2009**, *48*, 2549−2552.

(13) (a) Hardy, M.; Struch, N.; Topić, F.; Schnakenburg, G.; Rissanen, K.; Lützen, A. Stepwise Construction of Heterobimetallic Cages by an Extended Molecular Library Approach. *Inorg. Chem.* **2018**, *57*, 3507−3515. (b) Wang, Z.; Zhou, L.-P.; Zhao, T.-H.; Cai, L.-X.; Guo, X.-Q.; Duan, P.-F.; Sun, Q.-F. Hierarchical Self-Assembly and Chiroptical Studies of Luminescent 4d−4f Cages. *Inorg. Chem.* **2018**, *57*, 7982−7992.

(14) Carpenter, J. P.; McTernan, C. T.; Ronson, T. K.; Nitschke, J. R. Anion Pairs Template a Trigonal Prism with Disilver Vertices. *J. Am. Chem. Soc.* **2019**, *141*, 11409−11413.

(15) Dry, E. F. V.; Clegg, J. K.; Breiner, B.; Whitaker, D. E.; Stefak, R.; Nitschke, J. R. Reversible anion-templated self-assembly of [2 + 2] and [3 + 3] metallomacrocycles containing a new dicopper(I) motif. *Chem. Commun.* **2011**, *47*, 6021−6023.

(16) The tetrafluoroborate salt of **1** was also prepared from $[Cu^{I}(MeCN)_4](BF_4)$.

(17) Although cage **1** crystallized in the chiral space group $P2_13$, the structure was refined as a racemic twin (in addition to being a merohedral twin).

(18) (a) Kuang, S.-M.; Zhang, Z.-Z.; Wang, Q.-G.; Mak, T. C. W. Reaction of $[Cu_2(\mu\text{-}Ph_2Ppypz)_2(MeCN)_2](ClO_4)_2$ (Ph_2Ppypz = (2-diphenylphosphino-6-pyrazol-1-yl)pyridine) with $Fe(CO)_4^{2-}$ and X^- (X = Cl, I, $MeCO_2$ and pyrazolate). *J. Organomet. Chem.* **1998**, *558*, 131−138. (b) Kuang, S.-M.; Zhang, Z.-Z.; Wang, Q.-G.; Mak, T. Synthesis and reactivity of binuclear copper(I) complexes of 2-(diphenylphosphino)-6-(pyrazol-1-yl)pyridine (L^1). Crystal structures of $[Cu_2(\mu\text{-}L^1)_2(MeCN)_2][ClO_4]_2$, $[Cu_2(\mu\text{-}L^1)_2(\mu\text{-}\eta^1\text{-}C{\equiv}CPh)][ClO_4]\cdot CHCl_3\cdot H_2O$ and $[Cu_2(\mu\text{-}L^1)_2(\mu\text{-}Cl)][ClO_4]\cdot H_2O$. *J. Chem. Soc., Dalton Trans.* **1998**, 1115−1120. (c) Field, J. S.; Haines, R. J.; Parry, C. J.; Sookraj, S. H. Dicopper(I) complexes of the novel phosphorusbipyridyl ligand 6-diphenylphosphino-2,2′-bipyridyl. *Polyhedron* **1993**, *12*, 2425−2428. (d) Lilio, A. M.; Grice, K. A.; Kubiak, C. P. A Series of Dinuclear Copper Complexes Bridged by Phosphanylbipyridine Ligands: Synthesis, Structural Characterization and Electrochemistry. *Eur. J. Inorg. Chem.* **2013**, *2013*, 4016−4023.

(19) Although the signal for the phenyl protons H_6 of **B** was not observed at 298 K due to their intermediate rate of rotation on the NMR time scale, they were resolved when spectra were measured at 238 K, enabling all signals to be assigned (Figures S1 and S2).

(20) Bondi, A. Van Der Waals Volumes and Radii. *J. Phys. Chem.* **1964**, *68*, 441−451.

(21) Maglic, J. B.; Lavendomme, R.MoloVol: an easy-to-use program to calculate various volumes and surface areas of chemical structures and identify cavities. *ChemRxiv* **2021**, https://chemrxiv.org/engage/chemrxiv/articledetails/61473fb41df4a14d7d73c33b (accessed 2021−12−01).

(22) (a) Meng, W.; League, A. B.; Ronson, T. K.; Clegg, J. K.; Isley, W. C.; Semrouni, D.; Gagliardi, L.; Cramer, C. J.; Nitschke, J. R. Empirical and Theoretical Insights into the Structural Features and Host−Guest Chemistry of M_8L_4 Tube Architectures. *J. Am. Chem. Soc.* **2014**, *136*, 3972−3980. (b) Stiller, R.; Lehn, J.-M. Synthesis and Properties of Silver(I) and Copper(I) Helicates with Imine-Bridged Oligobipyridine Ligands. *Eur. J. Inorg. Chem.* **1998**, *1998*, 977. (c) Hamblin, J.; Childs, L. J.; Alcock, N. W.; Hannon, M. J. Directed one-pot syntheses of enantiopure dinuclear silver(I) and copper(I) metallo-supramolecular double helicates. *Dalton Trans* **2002**, 164−169. (d) Carvajal, M. A.; Novoa, J. J.; Alvarez, S. Choice of Coordination Number in d10 Complexes of Group 11 Metals. *J. Am. Chem. Soc.* **2004**, *126*, 1465−1477.

(23) Silver mainly exists as two isotopes, ^{107}Ag and ^{109}Ag (approximately 51.8% and 48.2%, respectively), which are both spin 1/2 and therefore NMR active, of which ^{109}Ag is usually preferred for probing the coordination environment of silver complexes due to its slightly higher sensitivity.

(24) (a) Hannon, M. J.; Bunce, S.; Clarke, A. J.; Alcock, N. W. Spacer Control of Directionality in Supramolecular Helicates Using an Inexpensive Approach. *Angew. Chem., Int. Ed.* **1999**, *38*, 1277−1278. (b) Mamula, O.; Monlien, F. J.; Porquet, A.; Hopfgartner, G.; Merbach, A. E.; von Zelewsky, A. Self-Assembly of Multinuclear Coordination Species with Chiral Bipyridine Ligands: Silver Complexes of 5,6-CHIRAGEN(o,m,p-xylidene) Ligands and Equilibrium Behaviour in Solution. *Chem.—Eur. J.* **2001**, *7*, 533−539. (c) Marquis, A.; Kintzinger, J.-P.; Graff, R.; Baxter, P. N. W.; Lehn, J.-M. Mechanistic features, cooperativity, and robustness in the self-assembly of multicomponent silver(I) grid-type metalloarchitectures. *Angew. Chem., Int. Ed.* **2002**, *41*, 2760−2764. (d) Keller, S.; Camenzind, T. N.; Abraham, J.; Prescimone, A.; Häussinger, D.; Constable, E. C.; Housecroft, C. E. Self-assembly of heteroleptic dinuclear silver(I) complexes bridged by bis(diphenylphosphino)-ethyne. *Dalton Trans* **2018**, *47*, 946−957.

(25) (a) Yue, N. L. S.; Jennings, M. C.; Puddephatt, R. J. Disilver(I) Macrocycles: Variation of Cavity Size with Anion Binding. *Inorg. Chem.* **2005**, *44*, 1125−1131. (b) Jin, G.-X.; Zhu, G.-Y.; Sun, Y.-Y.; Shi, Q.-X.; Liang, L.-P.; Wang, H.-Y.; Wu, X.-W.; Ma, J.-P. $[Ag{-}Ag]^{2+}$ Unit-Encapsulated Trimetallic Cages: One-Pot Syntheses and Modulation of Argentophilic Interactions by the Uncoordinated Substituents. *Inorg. Chem.* **2019**, *58*, 2916−2920. (c) Domoto, Y.; Abe, M.; Fujita, M. A Highly Entangled $(M_3L_2)_8$ Truncated Cube from the Anion-Controlled Oligomerization of a π-Coordinated M_3L_2 Subunit. *J. Am. Chem. Soc.* **2021**, *143*, 8578−8582. (d) Sawada, T.; Inomata, Y.; Shimokawa, K.; Fujita, M. A metal−peptide capsule by multiple ring threading. *Nat. Commun.* **2019**, *10*, 5687.

(26) The limited sensitivity of the ^{109}Ag isotope combined with the limited solubility of **2** prevented direct acquisition of the ^{109}Ag NMR spectrum within a reasonable time scale. To circumvent this limitation, a series of ^1H and ^{31}P NMR experiments were devised to investigate the effects of the coupling between the protons and phosphines of **2** and its Ag^I cations.

(27) The triflate salts of **3** and **4** were also prepared from $[Cu^{I}(MeCN)_4](OTf)$ and $Cd^{II}(OTf)_2$.

(28) (a) Parr, R. G.; Pearson, R. G. Absolute hardness: companion parameter to absolute electronegativity. *J. Am. Chem. Soc.* **1983**, *105*, 7512−7516. (b) Khammang, A.; Wright, J. T.; Meulenberg, R. W. Mechanistic insight into copper cation exchange in cadmium selenide semiconductor nanocrystals using X-ray absorption spectroscopy. *Nat. Commun.* **2021**, *12*, 438.

(29) Kieffer, M.; Bilbeisi, R. A.; Thoburn, J. D.; Clegg, J. K.; Nitschke, J. R. Guest Binding Drives Host Redistribution in Libraries of $Co^{II}_4L_4$ Cages. *Angew. Chem., Int. Ed.* **2020**, *59*, 11369−11373.

(30) Grancha, T.; Carne-Sanchez, A.; Hernandez-Lopez, L.; Albalad, J.; Imaz, I.; Juanhuix, J.; Maspoch, D. Phase transfer of rhodium(II)-based metal-organic polyhedra bearing coordinatively bound cargo

https://doi.org/10.1021/jacs.2c02261
J. Am. Chem. Soc. 2022, 144, 8467−8473

enables molecular separation. *J. Am. Chem. Soc.* **2019**, *141*, 18349−18355.
(31) (a) Casini, A.; Woods, B.; Wenzel, M. The Promise of Self-Assembled 3D Supramolecular Coordination Complexes for Biomedical Applications. *Inorg. Chem.* **2017**, *56*, 14715−14729. (b) Samanta, S. K.; Isaacs, L. Biomedical applications of metal organic polygons and polyhedra (MOPs). *Coord. Chem. Rev.* **2020**, *410*, 213181.
(32) Zhou, Y.; Li, H.; Zhu, T.; Gao, T.; Yan, P. A Highly Luminescent Chiral Tetrahedral $Eu_4L_4(L')_4$ Cage: Chirality Induction, Chirality Memory, and Circularly Polarized Luminescence. *J. Am. Chem. Soc.* **2019**, *141*, 19634−19643.
(33) (a) Keller, S.; Prescimone, A.; Bolink, H.; Sessolo, M.; Longo, G.; Martínez-Sarti, L.; Junquera-Hernández, J. M.; Constable, E. C.; Ortí, E.; Housecroft, C. E. Luminescent copper(I) complexes with bisphosphane and halogen-substituted 2,2′-bipyridine ligands. *Dalton Trans* **2018**, *47*, 14263−14276. (b) Safin, D. A.; Mitoraj, M. P.; Robeyns, K.; Filinchuk, Y.; Vande Velde, C. M. L. Luminescent mononuclear mixed ligand complexes of copper(I) with 5-phenyl-2,2′-bipyridine and triphenylphosphine. *Dalton Trans* **2015**, *44*, 16824−16832.
(34) (a) Ravaro, L. P.; Zanoni, K. P. S.; de Camargo, A. S. S. Luminescent Copper(I) complexes as promising materials for the next generation of energy-saving OLED devices. *Energy Rep* **2020**, *6*, 37−45. (b) Forero Cortés, P. A.; Marx, M.; Trose, M.; Beller, M. Heteroleptic copper complexes with nitrogen and phosphorus ligands in photocatalysis: Overview and perspectives. *Chem. Catalysis* **2021**, *1*, 298−338. (c) Housecroft, C. E.; Constable, E. C. TADF: Enabling luminescent copper(I) coordination compounds for light-emitting electrochemical cells. *J. Mater. Chem. C* **2022**, *10*, 4456−4482. (d) Zhang, Y.; Schulz, M.; Wächtler, M.; Karnahl, M.; Dietzek, B. Heteroleptic diimine−diphosphine Cu(I) complexes as an alternative towards noble-metal based photosensitizers: Design strategies, photophysical properties and perspective applications. *Coord. Chem. Rev.* **2018**, *356*, 127−146.

https://doi.org/10.1021/jacs.2c02261
J. Am. Chem. Soc. 2022, 144, 8467−8473